NUMERICAL SIMULATION OF CONDENSING AMMONIA IN PLATE HEAT EXCHANGERS USING CFD

Alexander Dietrich, Mario Nowitzki, Ron van de Sand and Prof. Dr.-Ing Jörg Reiff-Stephan
Faculty of Engineering and Natural Sciences
Technical University of Applied Sciences Wildau
15745, Wildau, Germany
E-mail: dietrich@th-wildau.de

KEYWORDS
Condensation, CFD, plate heat exchanger, refrigeration

ABSTRACT

For reasons of environmental compatibility and sustainability, the demand for more efficient heat exchangers is growing. The design of heat exchangers is based on experimentally determined correlations. For the use of heat exchangers under flow conditions that have not been researched yet, complex experimental investigations are necessary or a safety factor is applied. A third alternative is the investigation using Computational Fluid Dynamics (CFD). For this, however, it is necessary to generate an exact numerical model. Therefore, this study deals with the generation of a numerical model to simulate a condensation process of a widely used natural refrigerant, namely ammonia, within a plate heat exchanger (PHE). Based on the results of the pressure drop and the heat flow, the simulation's plausibility is checked with a validation test case. Thus, a statement about the accuracy of the CFD simulation is given.

INTRODUCTION

The consideration of condensation processes forms an integral part in the development of high-efficiency heat exchanger, such as heat pipes, nuclear industry reaction towers or refrigeration cycles (Huang et al. 2012) and is often the focus of attention in terms of reliability and efficiency aspects. Two-phase cooling schemes can deliver orders of magnitude enhancement in heat transfer coefficient compared to their single-phase counterparts. For that reason, condensation within heat exchangers is increasingly addressed across the literature in recent years (Kim and Mudawar 2013).

Especially with regard to vapor compression refrigeration systems (VCRS), predicting the condensation of the refrigerant within the condenser is crucial for the design of the overall system. However, as vapor and liquid flows occur simultaneously, the accurate estimation of the refrigerant flow characteristic, as well as the heat transfer, is more complex compared to the single-phase flow (Bhramara et al. 2009). Besides, condensers often consist of plate heat exchangers, which are generally more thermally efficient compared to their shell-and-tube counterparts (Huang et al. 2012). Due to the greater complexity of the channel geometry (Wang et al. 2007), which promotes a high degree of turbulence of the flow (Huang et al. 2012), the heat transfer estimation is additionally complex. Consequently, the accuracy of predicting the two-phase heat transfer in such non-circular channels by use of empirical correlations is often insufficient and may require experiments. Another approach is to use the Computational Fluid Dynamics to model the two-phase flow and heat phenomena in a PHE. In the field of fluid mechanics, such a model is most commonly developed using CFD, which can be applied to simulate the condensation process within a PHE. This allows an improved design of the VCRS and enables the theoretical evaluation of the system efficiency. Therefore, this work presents an approach towards the development of a CFD based numerical model for predicting the condensation process of ammonia in PHE. Furthermore, it describes the simulation and discusses its result based on a validation test case.

RELATED WORKS

Approximation of pressure drop and heat transfer during condensation of refrigerants in plate heat exchangers has gained attraction of researchers and many approaches are well described across the literature. Most authors found appropriate models though experimental investigations, which are widely applied for the development of VCRS. The empirical correlations describe the heat transfer and pressure drop of different refrigerants for different ranges of validity. For example, correlations for R134a were formulated by Yan et al. (Yan et al. 1999) and Zhang et al. (Zhang et al. 2019). Other authors, in turn, describe formulations for other refrigerants, such as R410a (Kuo et al. 2005) or hydrocarbons (Thonon and Bontemps 2002). García-Cascales et al. gives a large overview of correlations for single-phase and two-phase heat transfer (García-Cascales et al. 2007). Similar papers from Park and Hrnjak (Park and Hrnjak 2008) and Numrich and Müller (Numrich and Müller 2013) give general predictions for the condensation heat transfer and pressure drop in thin tubes.

Yet, a full understanding of the prediction of ammonia during condensation in plate heat exchanger is still lacking. Khan et al. (Khan et al. 2012) and Djordjevic and Kabelac (Djordjevic and Kabelac 2008) have already dealt with the formulation of correlation for the evaporation heat transfer and pressure drop of ammonia in plate heat exchangers. However, these correlations cannot be applied to condensation, since evaporation and condensation heat transfer are different (Soler 1996).

A problem with the simulation of two-phase flows is that locally different morphologies of the phase interface can

Communications of the ECMS, Volume 34, Issue 1,
Proceedings, ©ECMS Mike Steglich, Christian Mueller,
Gaby Neumann, Mathias Walther (Editors)
ISBN: 978-3-937436-68-5/978-3-937436-69-2(CD) ISSN 2522-2414

occur (Höhne and Vallée 2010). For that reason, an Algebraic Interfacial Area Density model (AIAD) was implemented based on the mixture model for the application in CFD (Höhne and Vallée 2010). In several studies, the results of the simulation with experimental data are compared (Höhne and Vallée 2010, Höhne and Lucas 2011). The developed model allows switching between correlations for the respective predominant morphology in the flow. Although the prediction of heat transfer and pressure drop of condensing refrigerant within PHEs has been addressed throughout the literature, the numerical approach still represents a challenge as the flow-describing conservation equations are not known/correct for many phenomena (e.g. multi-phase flow, turbulence, combustion) (Ferziger and Peric 2008). However, through the application of CFD, complex structures can be modeled and the condensation process could be observed within a wide range of applications.

In the two-phase model, the interfacial area density is one of the most important parameters (Wu et al. 1997). In industrial practice, however, the Sauter mean diameter is used to determine the interfacial area density, which is usually estimated through empirical correlations (Castellano et al. 2018). Another method for predicting the particle size distribution is through population balance equations PBE. PBE's are used to describe how the disperse phase develops as a population of entities in a continuous phase (Ramkrishna 2000). For an accurate description, however, a large number of population classes are required, which increases the computational effort (Lo and Zhang 2009). A simpler representation of the particle size distribution is obtained by a combination of breakup and coalescence models. The modification and development of new models for the interfacial area density is the topic of numerous publications (Yao and Morel 2004, Ishii and Kim 2001).

VALIDATION TEST CASE

The validation test case result data were taken from (Alfa Laval 2011) and are based on an ammonia water-glycol countercurrent plate heat exchanger condenser (Type Alfa Laval AlfaNova 76-80H). It is derived from the study carried out in (van de Sand et al. 2019) of which the collected data is used throughout this paper to estimate the numerical model deviation to the measurements.

Generally, the core of a plate heat exchanger is the stack of corrugated metal plates. In two separate circuits, refrigerant ammonia and coolant water-glycol are alternately passed through the plates. It is understood that the pressure drop, as well as the heat transfer, are significantly affected by the geometry and characteristics of the plate shapes (Focke et al. 1985). As illustrated in Figure 1, the chevron pattern embossings of two adjacent plates are arranged in opposite directions. Each plate is characterized by a chevron angle β, a wall thickness s, a corrugated pitch Λ, an amplitude b, a plate length L_P and a plate width W_P. The diameter of the ports which provide access to the flow passages on either side (inlet/outlet) is given by D_P.

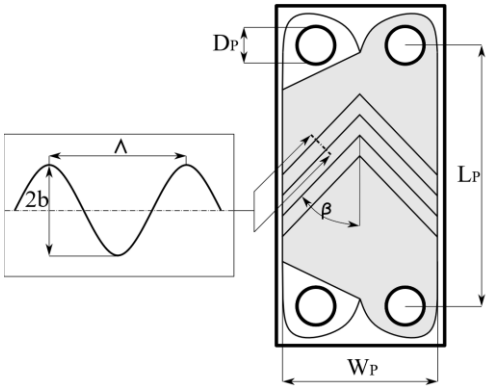

Figure 1: Corrugated Plate

To calculate the heat transfer and pressure drop for that validation test case, dimensionless number correlations for plate heat exchangers described by Martin (Martin 1996) are used. With a dimensional analysis, it can be shown that the Nusselt number Nu, the Reynolds number Re and the Prandtl number Pr are crucial parameters for the heat transfer and pressure drop (Stephan et al. 2019). In order to determine the dimensionless numbers, Martin (Martin 1996) shows, that the characteristic length can be replaced by the following hydraulic diameter, see equation 1.

$$d_h = \frac{4b}{\Phi} \tag{1}$$

Where Φ is the dimensionless parameter for the area enlargement factor and the result of the increased heat transfer surface due to the corrugated embossings. The dimensionless area enlargement factor definition can be seen in equation 2.

$$\Phi = \frac{1}{6} \cdot \left(1 + \sqrt{1 + X} + 4 \cdot \sqrt{1 + \frac{X^2}{2}}\right) \tag{2}$$

Where X is the dimensionless corrugation parameter, which can be determined from the heat exchanger plate corrugated pitch Λ and amplitude b, see equation 3 and Figure 1.

$$X = 2 \cdot \pi \cdot \frac{b}{\Lambda} \tag{3}$$

NUMERICAL MODEL

Grid generation

In this study, the CFD analysis is conducted based on a 3D model representing the continuum (channel) between two corrugated plates of the PHE. For the analysis of heat transfer and two-phase flow in a plate heat exchanger, it is possible to reduce the computational effort by simulating a single channel instead of the entire PHE. In

order to perform the simulation, the software StarCCM+ is used in this study. The inlet and outlet ports are extended so that the inlet and outlet boundary conditions have less effect on the flow conditions in the heat transfer area inside the channel.
The 3D model is meshed with polyhedral elements. In the channel, there are thin layer elements on the walls, in order to resolve the temperature boundary layer. In the segment where the corrugated embossings cross (main heat transfer area) the mesh is locally refined to better resolve the higher turbulence and thus heat transfer rates. Table 1 shows the mesh parameters. The mesh quality meets the recommendations of Lloyd and Espanoles (Lloyd and Espanoles 2002). In advance, the numerical model was tested on a tube condenser. A mesh-independent study was carried out for a tube condenser. Finally, the simulation results of the tube condenser were validated with an appropriate correlation from Stephan et al. (Stephan et al. 2019). The result of this latter previously investigation (mesh independence study) is a deviation of the numerical model of -49.9% for the pressure drop and -53% for the heat flow. Accordingly, a discretization error for the PHE simulation of approximately -2% for the pressure drop and approximately -10% for the heat transfer can be expected.

Table 1: Plate heat exchanger mesh parameters

Total layer thickness	0.4mm
Number of layers	3
Prism layer stretching	1.3
Base size	1.7mm
Min. face size	0.102mm
Cell element	Polyeder

Flow Model

To take into consideration the separation of the two-phase flow inside the heat exchanger channel, the gravity force must be included in the simulation model. The plate heat exchanger, which is examined in this study, is positioned vertical, so that the condensate can collect at the bottom of the heat exchanger and can be removed to the outlet nearby the bottom.
In order to model the two-phase flow within the PHE, the Eulerian Multiphase flow model is further applied, in which both the liquid and gas phase are considered as separate continua (Parekh and Rzehak 2018). For each of the two phases, separate conservation equations for mass and momentum are solved. The Algebraic Interface Area Density Model describes the interaction between the phases (Ishii and Hibiki 2010).
Due to the small temperature change close to the dew point, the simulation can be simplified. The gas phase is assumed as an ideal gas and the liquid phase with constant density. In the present study, the two-equation turbulence model k-ε is used to represent the turbulent properties of the flow.

Algebraic Interface Area Density Model

The Algebraic Interface Area Density Model (AIAD) was developed to capture different flow patterns in two-phase flow. Ishii and Hibiki (Ishii and Hibiki 2010) are giving an overview of different opportunities to mathematically describe two-phase flows. Depending on the gas/liquid volume fraction, three regimes are introduced of which each regime is provided with its own correlations and coefficients for the exchange of moments. Hence it is possible to switch between the correlations depending on the respective flow pattern locally. The three regimes are:

- Disperse bubbles in continuous liquid phase (bubbly regime)
- Liquid droplets in continuous gas phase (droplet regime)
- Separated Flow (free surface regime)

A blending function makes it possible to switch between regimes. This enables the localization and detection of the different regimes.
A regime is defined by its volume fraction. The bubbly regime is used for vapor volume fractions smaller 30 % and the droplet regime for vapor volume fraction greater than 70%. If the volume fraction is between 30 and 70%, the free surface regime is used. Figure 2 shows the relation between regimes and blending function.

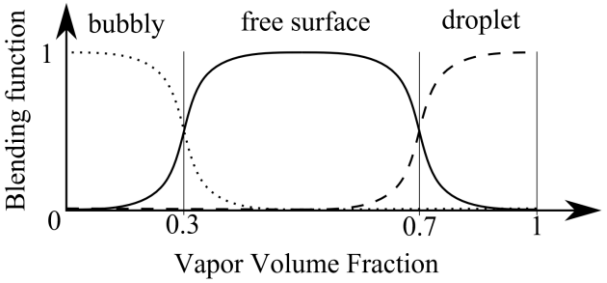

Figure 2: blending function for multiple flow regimes according to Porombka and Höhne (Porombka and Höhne 2015)

Generally, the momentum transport between phases must be modeled. The sum of the drag force and non-drag forces is the interfacial momentum transfer. The most crucial force for interfacial momentum transport is the drag force (Porombka and Höhne 2015).

Drag Force:
The drag force is the resistance on disperse particles in a continuous phase caused by different relative velocities to each other (Ishii and Hibiki 2010). The drag force is calculated as follows:

$$F_D = C_D \cdot A_{proj} \cdot |U_{rel}|^2 \cdot \frac{\rho}{2} \qquad (4)$$

where U_{rel} is the relative velocity between the phases, ρ the density of the continuum phase and A_{proj} the projected area of a particle. C_D is the drag force coefficient. In eq.

4 C_D and A_{proj} are unknown values that must be calculated. Thus, for the droplet and bubble regime, the correlation for C_D according to (Schiller and Naumann 1933) is used, which is suitable for flows consisting of small spherical bubbles/droplets. For the free surface regime, an adapted method of Štrubelj and Tiselj (Štrubelj Tiselj 2011) is used to calculate the interface drag coefficient.

$$A_{\alpha\beta} = \frac{A_{proj}}{V_{sphere}} \quad (5)$$

The Interfacial Area Density $A_{\alpha\beta}$, as shown in eq. 5, specifies the ratio of interfacial area A_{proj} per volume V_{sphere}. α and β represent the bubbly and droplet regime. For both the bubbly and droplet regime the spherical particle approach and for the free surface regime the mixture approach is used, see (Nowitzki 2020).

Surface Tension:
The surface tension is added to computation to ensure a correct fluid particle wall interaction. According to Hyvärinen et al., the surface tension for pure ammonia at 25°C is 0.021 mN/m (Hyvärinen et al. 2005).

Non-Drag Forces:
In addition to the Drag Force, which points in the opposite direction of the velocity vector, there are other forces perpendicular to the direction of flow affecting the momentum transfer. Ishii and Hibiki divide these forces into lift force, wall lubrication force and turbulent dispersion force (Ishii and Hibiki 2010). According to Legendre and Magnaudet, the lift force describes the lift/shear force on particles generally moving in a rotational flow (Legendre and Magnaudet 1998). In this study, the Tomiyama model (Tomiyama et al. 2002) is used for the bubbly regime and a constant coefficient of 0.25 is used for the droplet regime, following (Lance and Bateille 1991). Other Non-Drag forces than the lift force are neglected (Méndez et al. 2005).

Boundary conditions

Inlet condition:
In this study, according to the measurements in (Alfa Laval 2011) the ammonia gas mass flow value per single channel can be assumed as 0.003 kg/s.

Outlet condition:
The ammonia leaves the plate channel at a pressure of 1.16 MPa. The outlet values for temperature and the volume fraction of each phase that needs to be chosen are determined by a function, that is calculating the average value on a plane just before the outlet port.

Wall condition:
All heat transferring surfaces are assumed as a convective heat source to model the heat transfer on the coolant side. Heat transfer surfaces are all surfaces where the channel volume is touched by the plates. The remaining surfaces are assumed adiabatic, such as the wall of the inlet/outlet extensions or the sides of the plate channel. The temperature of the coolant rises logarithmically (Cartaxo and Fernandes 2011). For that reason, the average temperature of the coolant (water-glycol) is 24.4 °C and is calculated from the logarithmic mean of the temperatures given in (Alfa Laval 2011) at the inlet of 22 °C and at the outlet of 27 °C in the coolant circuit. The heat transfer coefficient of the coolant channel α_{WG} is calculated based on the correlation of Focke et al. (Focke et al. 1985) for water as:

$$\alpha_{WG} = 0.44 \cdot Re^{0.64} \cdot Pr^{0.5} \cdot \frac{\lambda_{WG}}{d_h} \quad (6)$$

where Pr is the Prandtl number, Re the Reynolds number, λ_{WG} is the thermal conductivity and d_h the is the hydraulic diameter, see equation 1. The Prandtl number consists of material properties of water-glycol. The Reynolds number is calculated as follows in equation 7:

$$Re_{WG} = \frac{U_{WG} \cdot d_h \cdot \rho_{WG}}{\mu_{WG}} \quad (7)$$

where ρ_{WG} is the density and μ_{WG} the dynamic viscosity of the coolant. The calculation of U_{WG} can be found in (Martin 1996).

Nusselt number

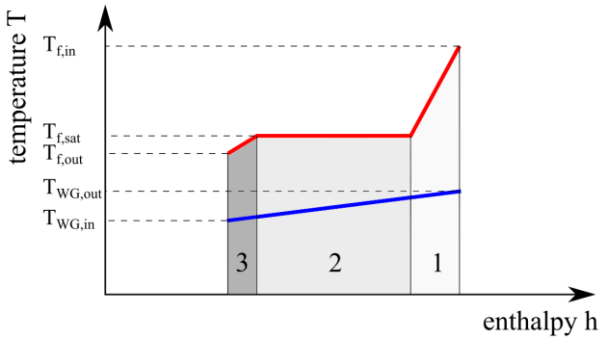

Figure 3: temperature profile of different heat transfer regions

It is necessary to specify the Nusselt number in order to simulate the heat transfer. As illustrated in Figure 3, the red graph represents the temperature drop of the refrigerant side and the blue graph the rise in temperature of the coolant side. $T_{f,in}$ and $T_{f,out}$ represent the inlet and outlet temperatures of the refrigerant circuit, $T_{WG,in}$ and $T_{WG,out}$ the inlet and outlet temperatures of the coolant circuit and $T_{f,sat}$ is the saturation temperature of the refrigerant. The whole heat transfer process is divided into three regions, as shown in Figure 3. Region 1: vapor desuperheating, region 2: saturation condensation, and region 3: liquid subcooling. Since the heat transfer rates vary a lot in these later different regions, it is necessary to treat them separately. Table 2 shows the used sources to determine the Nusselt number for each regime.

Table 2: Used Nusselt number for different regimes

Region	Nusselt number
1	Benchmark following (Hell 1992)
2	Determining according to calculation model from (Zhang et al. 2019)
3	Determining according to (Martin 1996)

Modeling the interaction length scale

Generally, dimensionless numbers in CFD, such as the Reynolds number, are based on the interaction length scale (ILS), which must be estimated. Usually, the Sauter mean diameter d_{32} can be used to specify the ILS (Zogg 1987). It is considered as an average of the particle size by volume and surface of the original bubble/droplet distribution (Siemens 2018, Zogg 1987). As it is difficult to determine d_{32} for an unknown flow, it is usually obtained from experiments. Additionally, the condensation process complicates the exact determination of d_{32}, since the amount of condensate increases with continuous flow and changes its Sauter diameter from inlet to outlet. One way of determining d_{32} is by assuming a logarithmic distribution of bubble/droplet diameters (Gnotke 2005). Hence, a simple logarithmic mean is calculated (see eq. 8). In conjunction with the maximum and minimum geometric boundaries, the ILS is given by:

$$l_{\alpha\beta} = d_{32} = \frac{(d_{max} - d_{min})}{\ln(d_{max}/d_{min})} \qquad (8)$$

Here, $l_{\alpha\beta}$ is the ILS of the respective regime. For spherical bubbles, the maximum possible diameter $d_{max} = 4.9$ mm is limited by the width of the plate channel. The minimum bubble diameter $d_{min} = 0.049$ mm is assumed to 1 % of d_{max}. Then the interaction length scale for the bubbly regime is calculated according to equation 8. The procedure for calculating the droplet Sauter mean diameter is different from the bubble region. Because the Reynolds number of the droplet regime is much higher than the Reynolds number in the bubbly regime, the droplet Sauter diameter is assumed as one-hundredth of the bubble Sauter mean diameter.

RESULTS AND DISCUSSION

The PHE being examined in this paper consists of 80 stacked plates. All geometric parameters of each plate are listed in Table 3. With these parameters, the calculation according to Martin (Martin 1996) results in a hydraulic diameter of d_h=4,3 mm for each plate channel.
For simplifications purposes, all roundings are removed from the 3D model. Furthermore, instead of a sinusoidal corrugated pattern, a trapezoidal one is modeled. All embossings in the distributor segments are removed and a uniform channel is assumed.

Table 3: plate parameters

Symbol	Meaning	Value
β	Chevron angle	60°
s	Plate thickness	0.4mm
Λ	Corrugated pitch	10mm
b	Amplitude	1.225mm
W_P	Plate width	192mm
L_P	Plate length	519mm
D_P	Port diameter	49mm

Figure 4 shows the cross-section of the modeled plate channel. The figure shows the locations in the cross-section where the liquid phase accumulates. Liquid collects due to gravity near the outlet at the lower end. It can also be seen in the figure that there are also small accumulations of the liquid phase in the main heat transfer area due to the enhanced condensation in that area.

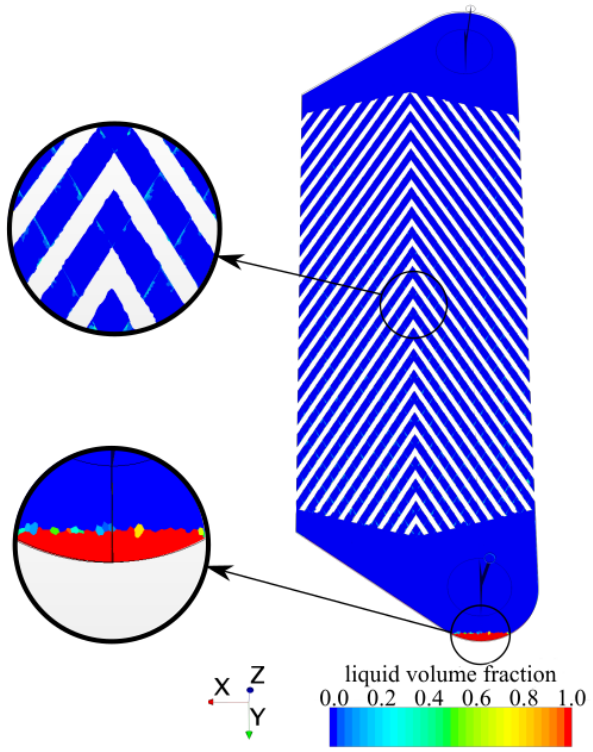

Figure 4: liquid volume fraction

The two characteristic parameters of every heat exchanger are the heat transfer and the pressure drop. Table 4 shows the comparison of the results of the simulation of the plate heat exchanger with the data obtained from Alfa Laval (Alfa Laval 2011). In the presented test case, the ammonia flows into the PHE at a temperature of $T_{f,in} = 75$ °C, condenses completely at $T_{f,sat} = 30$ °C and leaves the heat exchanger as a liquid at a temperature of $T_{f,out} = 28.1$ °C. At a system pressure of 1.16 MPa and a mass flow of 0.003 kg/s, this corresponds to a heat flow of $\dot{Q}_{real} = 3853\ W$ per plate channel (Alfa Laval 2011). In the simulation, the ammonia does not condense completely. This results in a

reduced heat flow of $\dot{Q}_{sim} = 1589\ W$, see Table 4. This corresponds to a deviation of -58.7 % for the heat flow.
The experimental data provide a pressure drop from inlet to outlet of $\Delta p = 779\ Pa$ (Alfa Laval 2011). However, the result of the simulation is $\Delta p = 519\ Pa$. Thus, the pressure drop is also below the experimental data with a deviation of -33.4 %.

Table 4: comparison of simulation and reality

Symbol	Simulation	Data from (Alfa Laval 2011)	Deviation
Δp	519Pa	779Pa	-33.4%
$\dot{Q}$	1589W	3853W	-58.7%

After the elimination of the systematic mistakes, the deviation of the mathematical model for the reduced heat flow is -53 % (see also mesh generation). An additional deviation of about 10 % can be expected due to the selected mesh. The deviation of -58.7 % in reduced heat flow between simulation and reality is therefore acceptable. The reason for this enormous deviation is the numerical model and the selected parameters. The correlations and benchmarks that are used for describing the Nusselt numbers of two-phase flow are fraught with uncertainty. As shown for example by Park and Hrnjak (Park and Hrnjak 2008), correlations are developed which can only predict numbers for the two-phase heat transfer within an accuracy of about ±20 %. Such correlations are simply unsuitable for engineering applications. As already mentioned, the flow describing conservation equations are also not correct. The sum of the coarse mesh, inaccurate Nusselt numbers and imprecise conservation equations lead to a deviation of -58.7 % for the heat flow.
The pressure drop and the amount of condensate that forms are related. If the amount of condensate increases, the pressure drop increases as well. While in (Alfa Laval 2011) the entire gas-phase condenses, in the simulation only 35 % condenses. This reduced condensate mass flow influences the pressure drop. A linear drop in pressure can be observed in the main heat transfer area of the PHE. When comparing the deviation of the simulation of the PHE with the mesh independence study, which was carried out in advance, it is of note that the pressure drop of the PHE is 16.5 % (-33.4 % for PHE, -49.9 % for tube) above expectations, but still below the value given in the PHE specification (Alfa Laval 2011).
Yet, there is one modeled parameter that has not been considered in the discussion. This parameter is the interaction length scale. The ILS has a significant impact on both pressure drop and heat transfer in the PHE. As mentioned above, ILS is related to the Reynolds number and thus to the pressure drop. The mass transfer is also influenced by the choice of the ILS.
In this study, only one constant is assumed to describe the ILS. However, this single constant is not enough to describe the entire flow in the PHE correctly. For that reason, a new model needs to be implemented to capture the local disparities.

Outlook

A numerical model for the simulation of condensation in the plate heat exchanger was created using the Eulerian Multiphase flow approach with the AIAD model for morphology detection. Necessary parameters, such as the Nusselt numbers and the ILS, were determined as a result of literature.
The results of the simulation show large deviations in the prediction of pressure drop (-33.4 %) and heat flow (-58.7 %). The ILS has a large impact on the pressure drop and the phase change. Therefore, the approach to determine the ILS should be redesigned and replaced by a model that detects local disparities.
The development of a new model for ILS is reasonable since condensation is an elementary component in highly efficient heat exchangers. For the design of highly efficient heat exchangers, a good prediction of the CFD is necessary to improve/optimize the design.
CFD can be a reliable alternative for the design of new heat exchangers once the mathematical simulation model has been validated. If this approach is applied in the design phase of new heat exchangers, another calculation model for the ILS should be used to advance its prediction accuracy as described in section “Related works”. The CFD simulation is a more general approach in contrast to literature empirically models and can be assigned of different geometries. But the biggest advantage of CFDs is that local detailed information can be extracted. This allows conclusions to be drawn about fouling effects, dead volume, hot spots, phase transition position within the process apparatus. Therefore, CFD is the suitable method for a comprehensive analysis of the flow.

REFERENCES

Alfa Laval. 2011. “AlfaFusion Plattenwärmeübertrager, Technische Spezifikationen” datasheet DEGLCPN-887(e)_2e Pos. 4.

Bhramara, P., Rao, V. D., Sharma, K. V. and Reddy, T. K. K. 2009. “CFD analysis of two phase flow in a horizontal pipe–prediction of pressure drop.” Momentum, 10, 476-482.

Cartaxo, S. J. and Fernandes, F. A. 2011. “Counterflow logarithmic mean temperature difference is actually the upper bound: A demonstration.” Applied Thermal Engineering, 31(6-7), 1172-1175.

Castellano, S., Sheibat-Othman, N., Marchisio, D., Buffo, A. and Charton, S. 2018. “Description of droplet coalescence and breakup in emulsions through a homogeneous population balance model”. Chemical Engineering Journal, 354, 1197-1207.

Djordjevic, E. and Kabelac, S. 2008. “Flow boiling of R134a and ammonia in a plate heat exchanger.” International Journal of Heat and Mass Transfer, 51(25-26), 6235-6242.

Ferziger, J. H., and Peric, M. 2008. “Numerische Strömungsmechanik.“ Springer-Verlag.

Focke, W. W., Zachariades, J. and Olivier, I. 1985. “The effect of the corrugation inclination angle on the thermohydraulic performance of plate heat exchangers” International Journal of Heat and Mass Transfer, 28, 1469-1479.

García-Cascales, J. R., Vera-García, F., Corberán-Salvador, J. M. and Gonzálvez-Maciá, J. 2007. “Assessment of boiling and condensation heat transfer correlations in the modelling

of plate heat exchangers." International Journal of Refrigeration, 30(6), 1029-1041.

Gnotke, O. 2005. "Experimentelle und theoretische Untersuchungen zur Bestimmung von veränderlichen Blasengrößen und Blasengrößenverteilungen in turbulenten Gas-Flüssigkeits-Strömungen" (Doctoral dissertation, Technical University of Darmstadt).

Hell, F. 1992. ´"Wärmeübertrager". Oldenbourg Industrieverlag, 2.

Höhne, T. and Lucas, D. 2011. "Numerical simulations of counter-current two-phase flow experiments in a PWR hot leg model using an interfacial area density model." International Journal of Heat and Fluid Flow, 32(5), 1047-1056.

Höhne, T. and Vallée, C. 2010. "Experiments and numerical simulations of horizontal two-phase flow regimes using an interfacial area density model." The Journal of Computational Multiphase Flows, 2(3), 131-143.

Huang, J., Sheer, T. J. and Bailey-McEwan, M. 2012. "Heat transfer and pressure drop in plate heat exchanger refrigerant evaporators." International Journal of Refrigeration, 35(2), 325-335.

Hyvärinen, A.-P., Raatikainen, T., Laaksonen, A., Viisanen, Y. and Lihavainen, H. 2005. "Surface tension and densities of H_2SO_4+NH_3+water solutions" Geophysical Research Letters, 32, L16806.

Ishii, M. and Hibiki, T. 2010. "Thermo-fluid dynamics of two-phase flow." Springer Science & Business Media.

Ishii, M. and Kim, S. 2001. "Micro four-sensor probe measurement of interfacial area transport for bubbly flow in round pipes". Nuclear Engineering and Design, 205(1-2), 123-131.

Khan, T. S., Khan, M. S., Chyu, M. C. and Ayub, Z. H. 2012. "Experimental investigation of evaporation heat transfer and pressure drop of ammonia in a 60 chevron plate heat exchanger." International Journal of Refrigeration, 35(2), 336-348.

Kim, S. M. and Mudawar, I. 2013. "Universal approach to predicting heat transfer coefficient for condensing mini/micro-channel flow." International Journal of Heat and Mass Transfer, 56(1-2), 238-250.

Kuo, W. S., Lie, Y. M., Hsieh, Y. Y. and Lin, T. F. 2005. "Condensation heat transfer and pressure drop of refrigerant R-410A flow in a vertical plate heat exchanger." International Journal of Heat and Mass Transfer, 48(25-26), 5205-5220.

Lance, M. and Bateille, J. 1991. "Turbulence in the liquid phase of a uniform bubbly air-water flow." Journal of Fluid Mechanics, 222, 95-118.

Legendre, D. and Magnaudet, J. 1998. "The lift force on a spherical bubble in a viscous linear shear flow." Journal of Fluid Mechanics, 368, 81-126.

Lloyd, G. and Espanoles, A. 2002. "Best practice guidelines for marine applications of computational fluid dynamics." WS Atkins Consultants and Members of the NSC, MARNET-CFD Thermatic Network: London, UK, 84.

Lo, S., and Zhang, D. 2009. "Modelling of break-up and coalescence in bubbly two-phase flows". The Journal of Computational Multiphase Flows, 1(1), 23-38.

Martin, H. 1996. "A theoretical approach to predict the performance of chevron-type plate heat exchangers." Chemical Engineering and Processing: Process Intensification, 35(4), 301-310.

Méndez, C. G., Nigro, N. and Cardona, A. 2005. "Drag and non-drag force influences in numerical simulations of metallurgical ladles." Journal of Materials Processing Technology, 160(3), 296-305.

Nowitzki, M. 2020. "Development and Validation of a Gas-Liquid Two-Phase Model for Industrial Computational Fluid Dynamics Application" Doctoral dissertation, Technical University Cottbus-Senftenberg.

Numrich, R. and Müller, J. 2013. "Filmkondensation reiner Dämpfe" VDI-Wärmeatlas, 11, 1011-1027.

Parekh, J. and Rzehak, R. 2018. "Euler–Euler multiphase CFD-simulation with full Reynolds stress model and anisotropic bubble-induced turbulence." International Journal of Multiphase Flow, 99, 231-245.

Park, C. Y. and Hrnjak, P. 2008. "NH3 in-tube condensation heat transfer and pressure drop in a smooth tube" International Journal of Refrigeration, 31(4), 643-651.

Porombka, P. and Höhne, T. 2015. "Drag and turbulence modelling for free surface flows within the two-fluid Euler–Euler framework." Chemical Engineering Science, 134, 348-359.

Ramkrishna, D. 2000. "Population balances: Theory and applications to particulate systems in engineering". Elsevier.

Schiller, L. and Naumann, A. 1933. "Über die grundlegenden Berechnungen bei der Schwerkraftaufbereitung" Zeitschrift Verein Deutscher Ingenieure, 77, 318-32.

Siemens. 2018. "STAR-CCM+ Dokumentation: Version 13.02".

Soler, J. M. 1996. "Cluster diffusion by evaporation-condensation." Physical Review B, 53(16), R10540.

Stephan, P., Kabelac, S., Kind, M., Mewes, D., Schaber, K., & Wetzel, T. 2019. "VDI-Wärmeatlas." Springer-Verlag.

Štrubelj, L. and Tiselj, I. 2011. "Two-fluid model with interface sharpening." International Journal for Numerical Methods in Engineering, 85(5), 575-590.

Thonon, B., & Bontemps, A. 2002. "Condensation of pure and mixture of hydrocarbons in a compact heat exchanger: experiments and modelling." Heat Transfer Engineering, 23(6), 3-17.

Tomiyama, A., Tamai, H., Zun, I. and Hosokawa, S. 2002. "Transverse migration of single bubbles in simple shear flows" Chemical Engineering Science, 57, 1849-1858.

van de Sand R., Falk C., Corasanti S. and Reiff-Stephan, J. 2019. "A data-driven fault diagnosis approach towards oil retention in vapour compression refrigeration systems," International IEEE Conference and Workshop in Óbuda on Electrical and Power Engineering (CANDO-EPE).

Wang, L., Manglik, R. M. and Sundén, B. 2007. "Plate Heat Exchangers: Design, Applications and Performance." International series on developments in heat transfer.

Wu, Q., Kim, S., Ishii, M. and Beus, S. G. 1998. "One-group interfacial area transport in vertical bubbly flow". International Journal of Heat and Mass Transfer, 41(8-9), 1103-1112.

Yan, Y. Y., Lio, H. C. and Lin, T. F. 1999. "Condensation heat transfer and pressure drop of refrigerant R-134a in a plate heat exchanger." International Journal of Heat and Mass Transfer, 42(6), 993-1006.

Yao, W. and Morel, C. 2004. "Volumetric interfacial area prediction in upward bubbly two-phase flow". International Journal of Heat and Mass Transfer, 47(2), 307-328.

Zhang, J., Kærn, M. R., Ommen, T., Elmegaard, B. and Haglind, F. 2019. "Condensation heat transfer and pressure drop characteristics of R134a, R1234ze (E), R245fa and R1233zd (E) in a plate heat exchanger" International Journal of Heat and Mass Transfer, 128, 136-149.

Zogg, M. 1987. "Einführung in die Mechanische Verfahrenstechnik". B. G. Teubner Stuttgart.